# Surface defects and the electronic structure of $SrTiO_3$ surfaces

Victor E. Henrich, G. Dresselhaus*, and H. J. Zeiger
*Lincoln Laboratory, Massachusetts Institute of Technology, Lexington, Massachusetts 02173*
(Received 12 December 1977)

The electronic properties of various types of $SrTiO_3$ surfaces have been studied by using ultraviolet-photoemission and electron-energy-loss spectroscopy, low-energy electron diffraction and Auger spectroscopy. Vacuum-fractured surfaces exhibit weak photoemission in the region of the bulk band gap, which is probably due to residual surface defects. When surface defects are produced by Ar-ion bombardment, a much stronger band of surface states appears in the band-gap region. These states arise from the creation of $Ti^{3+}$–O-vacancy complexes and are predominantly of *d*-electron character. Two surface defect phases are seen, one due to surface disorder and the other to changes in surface composition. The latter phase is stable under annealing to at least 1100 K. Exposure to $O_2$, however, depopulates the band-gap surface states on both vacuum-fractured and ion-bombarded surfaces. Models for the detailed structure of the defect surface states are discussed.

## I. INTRODUCTION

The properties of $SrTiO_3$ surfaces have been of considerable theoretical and experimental interest recently. Wolfram and co-workers[1,2] have calculated that intrinsic electronic surface states having *d*-electron character occur throughout much of the bulk band-gap region of insulating $SrTiO_3$ with a total density of about $10^{15}$ electrons/cm$^2$. A photoemission investigation of vacuum-fractured *n*-type $SrTiO_3$ surfaces by Powell and Spicer[3] indicated a maximum density of occupied surface states in the band gap of about $10^{13}$ electrons/cm$^2$. Subsequent calculations by Wolfram and Ellialtioğlu,[4] which included Coulomb repulsion among *d*-electrons, showed that the position of the *d*-band surface states depends on the position of the Fermi level, and that raising the Fermi level (by reduction of the sample, for example) pushes the surface states up into the bulk conduction band so that they remain largely unpopulated.

In this paper we report studies of the electronic properties of various types of $SrTiO_3$ surfaces,[5] including vacuum-fractured surfaces, surfaces with defects produced by Ar-ion-bombardment, and surfaces annealed both before and after ion bombardment, by using ultraviolet photoemission spectroscopy (UPS), low-energy electron diffraction (LEED), Auger-electron spectroscopy, and electron-energy-loss spectroscopy. On fractured surfaces we find a small density of occupied states in the bulk band gap, in general agreement with Powell and Spicer.[3] When defects are produced on the surface, however, large changes in the electronic structure occur in the region of the valence bands, and a relatively narrow band of defect surface states appears in the bulk band gap. At low defect densities, the electronic states produced at the surface are associated with surface disorder. As the defect density is increased, a second surface phase, associated with changes in surface stoichiometry, occurs. Upon adsorption of $O_2$, the band-gap surface states are depopulated in a manner analogous to defect surface states on $TiO_2$.[6] Unlike $TiO_2$, annealing the surface of $SrTiO_3$ to about 1100 K does not remove the band-gap surface states, even though it does produce a well-ordered surface (as determined by LEED). The band-gap surface states appear to arise from $Ti^{3+}$ ions associated with O vacancies.

## II. EXPERIMENTAL PROCEDURE

The $SrTiO_3$ samples were cut from an insulating, single-crystal boule obtained from NL industries, Inc. Mass spectroscopic analysis showed the major impurities to be 0.76 at.% C and 0.09 at.% B, relative to Sr. Although the crystal was pulled from a melt that contained 500-ppm $Ta_2O_5$ by weight (corresponding to 0.04 at.% Ta, relative to Sr), no estimate for Ta was possible by mass spectroscopic analysis because of signals arising from Ta components in the spectrometer. Samples for vacuum-fracturing were rods $4 \times 4$ mm$^2$ in cross section, with a [100] axis along the length of the rod. Samples with (100) surfaces were oriented ($\pm 2°$), cut and polished down to 1/2-$\mu$m diamond paste. The polished surfaces were then etched in $H_3PO_4$ for 1 h at 373 K to remove work damage. All samples were reduced in the ultrahigh-vacuum system used for the photoemission, LEED, Auger, and energy-loss measurements (base pressure about $1 \times 10^{-10}$ Torr, $O_2$ partial pressure about $5 \times 10^{-13}$ Torr) by heating to about 1000 K for several hours; the reduced samples were deep blue or blue gray in color. Samples reduced under these conditions are *n*-type

 ©1978 The American Physical Society

with a maximum carrier concentration of the order of $10^{19}$ electrons/cm.[3,7] At that carrier concentration, the width of a depletion or accumulation layer at the surface produced by a change in surface potential would be about 500 Å.[8] Since our experimental techniques sample only the first 5–30 Å, the positions of Fermi levels, band edges, work function, etc., determined from them will be due only to the surface, with no significant contribution from bulk levels.

Bombardment with Ar ions incident at about 20° to the sample surface was used to produce surface defects (e.g., disorder, changes in stoichiometry). For most of the experiments reported here the ion energy was 500 eV and the ion flux density was about 5 $\mu$A/cm$^2$. A series of Ar-ion bombardments was used to increase the defect density in a controlled manner, with bombardment intervals ranging from 5 sec to 10 min. After each bombardment, the residual Ar gas was pumped out of the system before spectroscopic measurements were made. A similar procedure was used when the samples were exposed to $O_2$. Samples were annealed in vacuum by heating to about 1100 K by electron bombardment of either the front or the back of the sample, depending on sample geometry.

All electron spectra were measured with a double-pass cylindrical-mirror electron spectrometer. For photoemission and energy-loss spectra, the spectrometer was run in the retarding mode with pass energies of 10 and 50 eV, respectively; for Auger spectra, it was run in the nonretarding mode. The photoemission spectra were excited with the He I line (21.2 eV) emitted by a microwave discharge lamp. The lamp also produced a He line at 23.1 eV whose intensity, determined from UPS spectra of metallic samples, was 1.4% of that of the 21.2-eV line; when necessary, the data were corrected for the presence of the satellite line. The photons were incident at about 70° from the normal to the sample surface, and the axis of the electron spectrometer was along the normal to the sample surface. The location of the Fermi level $E_F$ for photoemission spectra was determined from the spectrum of atomically clean Au. The density of photoemitted electrons $n(E)$ was recorded vs their kinetic energy, and the latter was then converted to the initial-state energy, $E$, for the electrons in the sample. The zero of initial-state energy was taken as either $E_F$ or the upper edge of the valence band $E_v$. The system resolution for photoemission measurements was about 0.2 eV.

Electron-energy-loss spectra were excited with an electron gun coaxial with the spectrometer; the incident-electron energy was 100 eV for all spectra reported here in order to maximize the sensitivity to surface features. A modulation of 0.4 eV peak to peak was applied to the electron gun cathode in order to eliminate Auger features from the spectra. The first derivative of the emitted electron distribution $dn(E)/dE$ was recorded vs energy loss $E_L$. The total system resolution for energy-loss measurements was about 0.75 eV. The same electron gun was used to excite Auger spectra, with an incident-electron energy of 2000 eV; a modulation of 3 eV peak to peak was applied to the outer cylinder of the spectrometer for those spectra. Low-energy-electron-diffraction (LEED) patterns were displayed on a four-grid 180° LEED optics with a coaxial electron gun.

## III. VACUUM-FRACTURED SURFACES

A schematic diagram of the approximate bulk electron energy level structure of $SrTiO_3$ is shown in Fig. 1. The levels and bands are labeled with the atomic levels from which they are predominantly derived. The bulk Fermi level in reduced samples lies just below the Ti($3d$) conduction band. The bulk band gap in $SrTiO_3$ at room temperature is 3.17 eV.[9] In UPS experiments using a photon energy of 21.2 eV, no bands below the O($2p$) valence band are accessible.

In order to study the electronic properties of stoichiometric $SrTiO_3$ surfaces, a number of samples were fractured in ultrahigh vacuum. Published x-ray photoemission studies[10] of $SrTiO_3$ surfaces that had been fractured in air showed them to have the same composition as the bulk, and we assume the same to be true of vacuum-fractured surfaces. Fractured surfaces are generally slightly curved, with their average surface normal within about ±15° of the [100] axis (see Fig. 3.14 of Ref. 11). The quality of the LEED

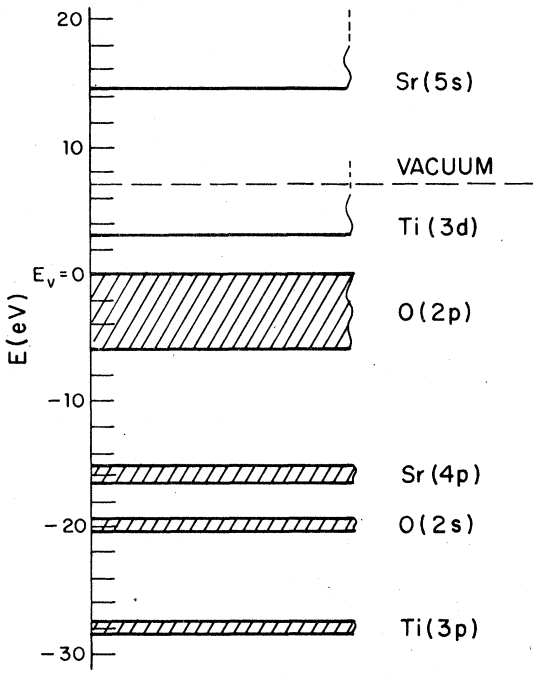


FIG. 1. Schematic energy-level diagram for $SrTiO_3$.

patterns varied for different fractures, with spots always visible but never as sharp or bright as those from an annealed surface.

Figure 2(a) shows the photoemission spectrum for a good fracture (i.e., relatively sharp LEED patterns, fairly flat surface). Here the initial energy $E$ is measured relative to the Fermi level $E_F$. The valence-band emission ($3\ \text{eV} \lesssim E \lesssim 9\ \text{eV}$) exhibits two peaks arising from the orbitals of the O($2p$) electrons,[1] the higher-lying one predominately from the $\pi$ orbitals and the lower one from the $\sigma$ orbitals. The Fermi level lies about 3.1 eV above the top of the valence band, which places it within 0.1 eV of the bottom of the conduction band. Since that is also the position of the Fermi level in the bulk for heavily reduced material, there does not appear to be any appreciable band bending on a vacuum-fractured surface.

Some electron emission is seen from the region of the bulk band gap in Fig. 2(a). In order to determine the emission intensity accurately, the "ghost" spectrum of the valence band generated by the 23.1-eV line must be subtracted from the spectrum of Fig. 2(a); this has been done in Fig. 2(b). The corrected band-gap emission exhibits a peak at about 1.7 eV above $E_v$. The amplitude of this peak varies from one fracture to another by a factor of 3 or 4; the one shown in Fig. 2 is near the lower limit. An estimate

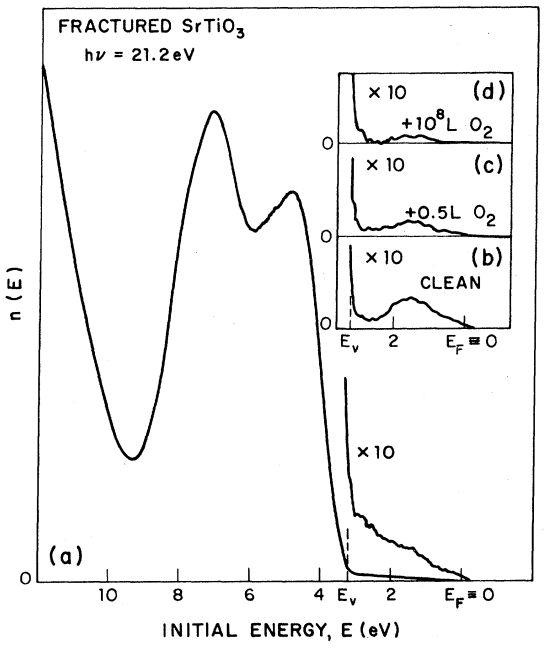


FIG. 2. Ultraviolet photoemission (UPS) spectra, $n(E)$ vs initial-state energy $E$ measured from the Fermi level $E_F$ for vacuum-fractured $SrTiO_3$(100) (a) before and (b)–(d) after subtraction of 23.1 eV "ghost" spectrum; (b) as fractured, (c) after exposure to 0.5 L (1 langmuir $=10^{-6}$ Torr sec) $O_2$, (d) after exposure to $10^8$ L $O_2$.

of the density of states that contributes to this emission can be made by comparing the area under the photoemission peak in the gap with that under the valence-band peaks. We assume that the valence-band photoemission intensity is of bulk origin and is given by

$$I_b = CAn_b|M_b|^2 \int_0^\infty e^{-z/\lambda_{\text{eff}}}\,dz \ , \tag{1}$$

where $C$ is a constant, $A$ is the surface area sampled, $n_b$ is the bulk density of electrons contributing to the peak, $M_b$ is the matrix element for photoexcitation of those electrons, $z$ is the distance below the surface, and $\lambda_{\text{eff}}$ is an effective electron mean-free path that depends on the electron energy and the spectrometer geometry. For our analyzer $\lambda_{\text{eff}} \approx \lambda \cos\theta$, where $\theta = 42.3°$ is the mean acceptance angle of the analyzer, measured from the surface normal, and $\lambda$ is the energy-dependent electron mean-free path.[12] For emission from purely surface states, we assume that the intensity is given by

$$I_s = CAn_s|M_s|^2 \ , \tag{2}$$

where $n_s$ is the surface density of electrons contributing to the peak and $M_s$ is the corresponding matrix element.

Since the valence-band emission arises predominantly from the six $2p$ electrons of the O atoms, and since there are three O atoms per unit cell,

$$n_b = (6 \times 3)/(a_0)^3 \ , \tag{3}$$

where $a_0$ is the lattice constant of $SrTiO_3$. If we wish to determine a surface or bulk density of electrons contributing to some other photoemission peak by comparing its intensity to that of the valence band, we must assume values for $\lambda_{\text{eff}}$ and for the ratios of the squares of the matrix elements for emission from the two bands. Values of $\lambda_{\text{eff}}$ can be determined to within about a factor of 2.[12] The matrix elements for these transitions are not known, and, since the valence band is predominantly O derived while the surface state is believed to be Ti derived, they cannot be assumed equal *a priori*. However, a good idea of their ratio can be obtained from photoemission spectra from vacuum-fractured $Ti_2O_3$,[6] which has an O derived valence band analogous to that in $SrTiO_3$ and a filled Ti-derived conduction band which lies about 3 eV above the valence band. By applying Eq. (1) to photoemission spectra taken under the same conditions as for $SrTiO_3$, we find a value of $\sim 0.7$ for the ratio of the squares of the conduction band to valence band matrix elements for $Ti_2O_3$. We have therefore taken the matrix elements for the valence band and the band-gap surface state in $SrTiO_3$ to be equal to each other.

If we consider the bandgap emission in Fig. 2(b) to be of surface origin and describe its intensity by Eq. (2), we find that

$$n_s \approx 5 \times 10^{13} \text{ electrons/cm}^2 ,$$

which corresponds to about 1 electron in every ten surface unit cells. This is somewhat larger than the upper limit for the surface-state density of about $1 \times 10^{13}$ electrons/cm$^2$ determined by Powell and Spicer.[3] We must also consider the possibility that the band-gap emission could arise from bulk states. Again assuming the same matrix elements for emission from both band-gap and valence-band states, a band-gap peak of the magnitude shown in Fig. 2(b) would correspond to a bulk density of

$$n_b \approx 4 \times 10^{20} \text{ electrons/cm}^3 .$$

This is more than an order of magnitude larger than the carrier concentration expected from O vacancies in these samples, and it is about five times larger than the highest concentration measured by Yamada and Miller[7] in samples reduced at 1700 K.

The rather high C concentration seen in our samples by mass spectroscopic analysis raises the question of whether the observed band-gap emission could be due to C electrons. Normalizing the bulk density above to the density of Sr atoms gives 0.023 electrons/Sr atom. Since the ratio of C to Sr atoms was measured to be 0.0076, three electrons on each C atom would have to contribute if the band-gap emission were due to C atoms; this is not an unreasonable number.

However, an argument against attributing the band-gap emission to bulk states is provided by the changes in emission upon exposure of a fractured surface to $O_2$. As shown in Figs. 2(c) and 2(d), as little as 0.5 L (1 langmuir L $\equiv 10^{-6}$ Torr sec) of $O_2$ reduces the intensity of the band-gap emission peak by a factor of 2, and after $10^8$ L exposure the peak is an order of magnitude smaller than on the newly fractured surface. This behavior is strongly indicative of surface states.

The low-energy region of the electron-energy-loss spectrum for a vacuum-fractured $SrTiO_3$ surface is shown in Fig. 3(a). The three strong features corresponding to peaks in $n(E)$ at $E_L = 5.5$, 10.5, and 14.0 eV occur at nearly the same energies as the three peaks seen in the same region of the loss spectra of $TiO_2$ and $Ti_2O_3$.[6] A fourth, weak feature is present at $E_L = 7.0$ eV. The 5.5, 7.0, and 10.5 eV transitions are probably O-to-Ti cross excitations. The peak at $E_L = 14.0$ eV could also be due to an O-to-Sr cross exitation; the fact that its shape is very similar to that of the 13.5-eV peak in $TiO_2$, however, makes an O-to-Ti transition more likely. None of the major features in this region of the energy-loss spectrum are believed to arise from plasma oscillations, since the calculated value of the bulk plasmon energy is 26.4 eV. No features below $E_L = 5.5$ eV are present in the energy-loss spectra of fractured material.

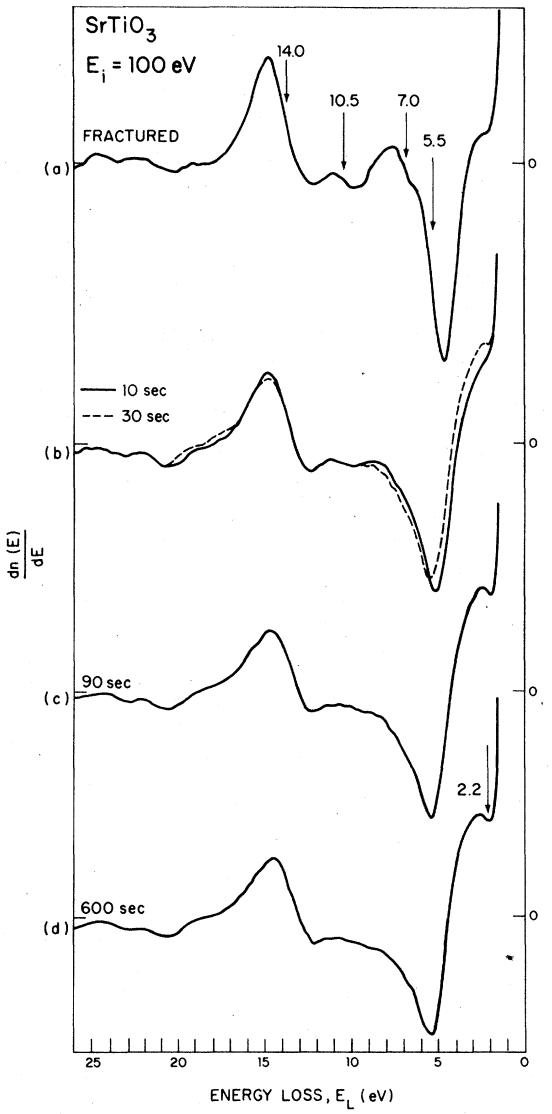


FIG. 3. Electron-energy-loss spectra (derivative of the secondary-electron energy distribution $dn(E)/dE$ vs energy loss $E_L$) for (a) vacuum-fractured $SrTiO_3(100)$, and for the same surface after 500-eV Ar-ion bombardment for (b) 10 sec (solid curve) and 30 sec (dashed curve), (c) 90 sec, and (d) 600 sec. Arrows indicate the location of peaks in $n(E)$.

Annealing of vacuum-fractured surfaces at about 1100 K for a few minutes improves the quality of the LEED patterns, but there is little effect on the other electron spectra. The Auger spectra indicate the same surface composition after annealing, and the energy-loss spectra are essentially unchanged. The only changes apparent in the photoemission spectra are a sharpening of the valence-band structure and subtle changes in the band-gap emission; the overall intensity of the band-gap emission is roughly the same before and after annealing.

## IV. DEFECT SURFACE STATES

When the surface of $SrTiO_3$ is bombarded by electrons or ions, its electronic structure changes. We have not studied the effects of electron bombardment in detail, but we have seen changes in the energy-loss spectra for $E_L \lesssim 2$ eV after several minutes of bombardment with the 100 eV electron beam used for those measurements.[13] To avoid such artifacts, each energy-loss spectrum was taken in 30 sec. Auger spectra were also recorded rapidly, with each spectrum taken in approximately 20 sec; no changes are observed in the Auger spectra during that time.

We have focused our attention on the creation of surface defects by ion bombardment. As a result of ion bombardment new electronic states appear in the bulk band gap, the structure of the valence band is modified, and the positions of both the Fermi level and the vacuum level change. Above a certain defect density, the atomic composition of the surface also changes. In the following section we will discuss the changes in surface electronic properties as a function of the extent of ion bombardment. The methods used were the same as in our study of defect surface states on $TiO_2$.[6]

### A. Creation of defects by ion bombardment

Defects were produced on vacuum-fractured surfaces by bombardment with 500-eV Ar ions for periods ranging from 5 sec to a total time greater than 10 min. Figure 4 shows the photoemission spectra for a fractured surface and for the same sample after total bombardment times of 10, 90, and 600 sec; bombardment for times longer than 600 sec produced no additional changes. The spectra of Fig. 4 are all referenced to a common Fermi level. The most striking features of the spectra are the reduction in intensity of the valence-band emission and the appearance of an emission band in the bulk band gap with bombardment. In addition, the separation between the two peaks in the valence-band emission decreases and the peaks broaden, and the Fermi level moves away from the valence band as the band-gap states are produced. The number of electrons contributing to the band-gap emission after equilibrium has been reached at long bombardment times has been calculated from the relative intensities of the band-gap and valence-band photoemission peaks. Assuming that the states are confined to the surface, the surface density is about $1 \times 10^{15}$ electron/cm$^2$, or about 1.5 electrons per surface unit cell.

Figure 5 plots the location of both the peak in the emission from the band-gap surface states $E_s$ and the Fermi level $E_F$, with respect to $E_v$ versus the normalized intensity of the band-gap emission. It also shows $\Delta\Phi$, the difference between the work function $\Phi$

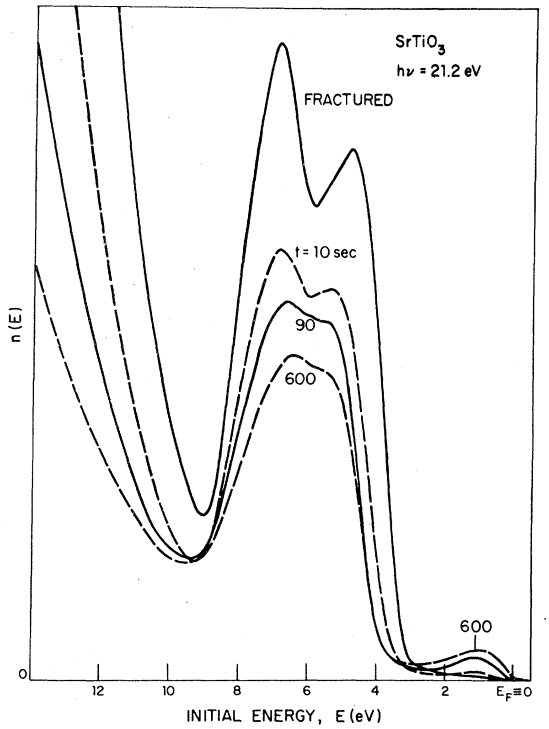


FIG. 4. UPS spectra for vacuum-fractured $SrTiO_3(100)$ for various 500-eV Ar-ion bombardment times. Spectra are aligned at $E_F$.

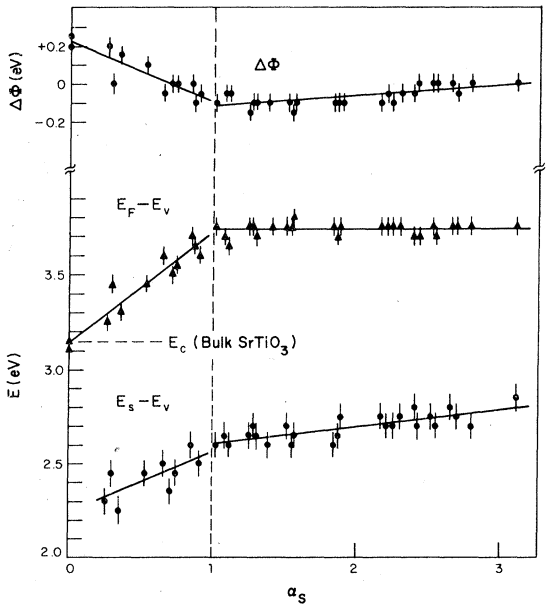


FIG. 5. Work-function change ($\Delta\Phi$), Fermi level ($E_F - E_v$), and position of UPS surface-state peak ($E_s - E_v$) vs normalized intensity of UPS surface-state peak ($\alpha_s$) for 500-eV Ar-ion bombardment of three vacuum-fractured $SrTiO_3(100)$ surfaces.

(measured from the low-energy cutoff of the photoemission spectrum), and the equilibrium value of $\Phi$ at long bombardment times. The abscissa $\alpha_s$, which is a measure of the number of occupied surface states, is the area under the band-gap photoemission peak, with a linear background subtracted, normalized to its value where the data change slope. (This is the same type of abscissa used in Ref. 6, and it has been normalized in a similar manner.) With increasing bombardment times $t$, $\alpha_s$ increases most rapidly for small $t$, eventually becoming constant; its functional dependence on $t$ (in seconds) is found to be approximately

$$\alpha = 2.7(1 - e^{-t/94}) \tag{4}$$

for the bombardment conditions given above. The position of the bottom edge of the bulk conduction band $E_c$ in $SrTiO_3$ is indicated by the horizontal dashed line. The points represent data from runs on three different vacuum-fractured surfaces.

The band-gap photoemission peak that results from Ar-ion bombardment does not appear to have the same origin as the one seen for vacuum-fractured surfaces. Although the amplitude of the band-gap peak on vacuum-fractured surfaces can vary by a factor of four from one surface to another, its energy maximum always occurs 1.7–1.8 eV above $E_v$. The peak produced by Ar-ion bombardment, however, is located 2.2–2.3 eV above $E_v$ even at $\alpha_s \approx 0$.

The three quantities plotted in Fig. 5 all exhibit discontinuities in slope at $\alpha_s = 1$. The solid lines shown are least-squares linear fits to the data for $\alpha_s < 1$ and for $\alpha_s > 1$. The most striking change is in $(E_F - E_v)$, which rises linearly with $\alpha_s$ for $\alpha_s < 1$, and then remains constant for $\alpha_s > 1$. The rate at which the peak of the band-gap surface-state emission moves away from the valence band decreases by a factor of 3.5 for $\alpha_s > 1$. The work function decreases on initial ion bombardment ($\alpha_s < 1$), then increases slightly for longer bombardment times.

Auger-electron spectra were used to monitor changes in the surface composition with Ar-ion bombardment. The results for the three runs of Fig. 5 are shown in Fig. 6, where the ratios of the peak-to-peak amplitude of features in the first-derivative Auger electron spectra are plotted vs $\alpha_s$ for O-to-Ti and Sr-to-Ti. The Auger peaks used are O (510 eV), Ti (318 eV), and Sr (average of 63, 79, and 104 eV), and the ratios have been normalized to 1 for $\alpha_s < 1$. The Ti (416 eV) peak was not used because its shape changes upon ion bombardment. For $\alpha_s < 1$, the O-to-Ti and Sr-to-Ti ratios in each run either remain constant or increase slightly with $\alpha_s$. For $\alpha_s > 1$, both ratios decrease linearly with $\alpha_s$, indicating a relative loss of both O and Sr with ion bombardment. Such a delayed onset of the change in surface composition was also seen for $TiO_2$.[6] As in the case of $TiO_2$, the LEED pattern begins to degrade immediately on bombardment,

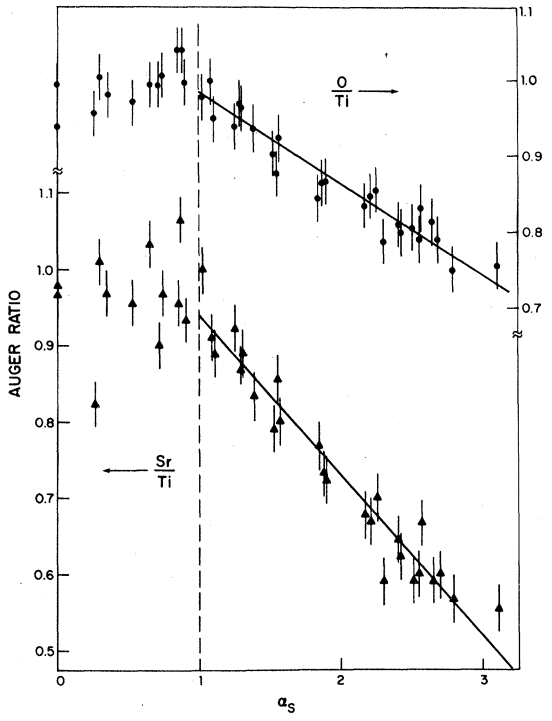


FIG. 6. Ratio of Sr-to-Ti and O-to-Ti Auger peaks (peak-to-peak amplitude in $dn(E)/dE$) vs $\alpha_s$ for 500-eV Ar-ion bombardment of vacuum-fractured $SrTiO_3(100)$ surface. The solid lines for $\alpha_s > 1$ are least-squares linear fits to the data.

indicating that the surface disorders without appreciable change in stoichiometry for $\alpha_s < 1$.

In order to get a rough idea of the change in the atomic composition of the surface region produced by Ar-ion bombardment, we have assumed that a uniform layer extending a distance $d$ below the surface has an altered composition, and that the remainder of the sample is $SrTiO_3$. (Such a model is admittedly weak since electron mean-free paths are comparable to lattice spacings[12]; we will consider more detailed models below.) We have neglected backscattering and diffraction[14] and have assumed $d$ values of 1, 2, and 3 lattice constants (4, 8, and 12 Å). Initially, we also assume that the volume concentration of Ti atoms $n_{Ti}$ is the same in the altered layer as in bulk $SrTiO_3$. The resulting compositions for long bombardment times ($\alpha_s > 3$) are listed in the left half of Table I. Since these compositions indicate a density of Ti ions somewhat larger than in $SrTiO_3$, we have recomputed the altered composition assuming that the Ti density in the altered layer is twice that in $SrTiO_3$; the resultant compositions are given in the right half of Table I. The surface composition is seen to be fairly insensitive to the Ti density, and for a thickness greater than one lattice constant it is approximately $SrTi_2O_4$. If one as-

TABLE I. Surface composition of Ar-ion-bombarded $SrTiO_3$ determined from Auger data.

| $d$(Å) | $n_{Ti}(z<d)\equiv n_{Ti}(z>d)$ | $n_{Ti}(z<d)\equiv 2n_{Ti}(z>d)$ |
|---|---|---|
| 4 | $Sr_{0.85}Ti_2O_{3.1}$ | $Sr_{0.8}Ti_2O_{3.8}$ |
| 8 | $Sr_{1.05}Ti_2O_{4.1}$ | $Sr_{0.95}Ti_2O_{4.3}$ |
| 12 | $Sr_{1.1}Ti_2O_{4.3}$ | $Sr_{1.05}Ti_2O_{4.4}$ |

sumes that the Sr and O ions retain their valences of +2 and −2, respectively, this implies that most of the Ti ions in the surface layer are $Ti^{3+}$ instead of the $Ti^{4+}$ of bulk $SrTiO_3$. Thus the band-gap surface state presumably consists of the $3d$ electrons on the $Ti^{3+}$ ions, as is the case for ion-bombarded $TiO_2$.[6] Detailed atomic models for the surface structure, which will be discussed in Sec. V B below, also indicate the presence of $Ti^{3+}$ ions at the surface.

Additional evidence for the $d$-electron nature of the band-gap surface state is given by the behavior of the 416-eV Ti Auger peak. As mentioned above, this peak was not used in surface composition analysis because its shape changes upon ion bombardment.[15] The region of the Auger spectrum from 350 to 450 eV for both vacuum-fractured $SrTiO_3$ and $Ti_2O_3$ is shown in Fig. 7(a). The Ti (416-eV) structure is seen to be composed of two peaks, which have been labeled $A$ and $B$ on the $SrTiO_3$ spectrum. When $SrTiO_3$ is bombarded, the amplitude of peak $A$ increases and that of peak $B$ decreases, until at long bombardment times the Auger spectrum looks roughly like that for vacuum-fractured $Ti_2O_3$. As peak $A$ increases, a new peak also appears at about 450 eV. Figure 7(b) plots the ratio of the amplitude of peak $A$ to peak $B$ vs $\alpha_s$; the solid line is a least-squares linear fit to the data for all $\alpha_s$. The horizontal dashed lines indicate the ratios of peak $A$ to peak $B$ measured for vacuum-fractured surfaces of $SrTiO_3$, $TiO_2$, and $Ti_2O_3$. (The values of these ratios depend on experimental conditions such as modulation voltage, resolution, and analyzer geometry; all of these variables were the same for the data plotted here.) The ratio varies smoothly with $\alpha_s$, exhibiting none of the discontinuities in slope seen in all of the other variables; it thus appears to have the same origin as the band-gap surface-state peak. The region of the Auger spectrum near 416 eV arises from $L_2M_{2,3}M_{2,3}$ ($2p_{1/2}3p3p$) transitions, which, since they involve the outermost Ti levels, should be sensitive to population of the Ti($3d$) levels. The ratio of the two peaks appears to be a measure of the concentration of $Ti^{3+}$ ions, ranging from values of 0.2 to 0.5 for materials with no $3d$ electrons to values greater than 2 for materials containing all $Ti^{3+}$ ions.

The changes in the energy-loss spectra due to Ar-ion bombardment of a vacuum-fractured surface are

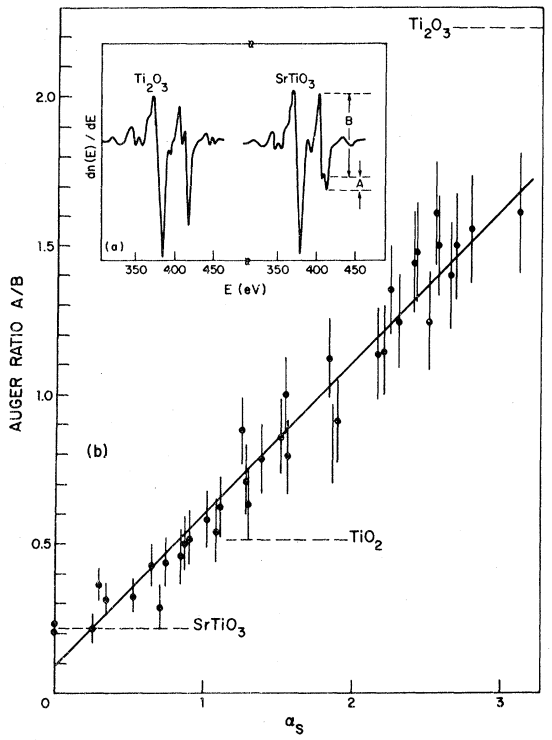


FIG. 7. (a) Ti Auger spectra for vacuum-fractured $Ti_2O_3$ and $SrTiO_3$, (b) ratio of amplitude of Auger features $A/B$ in (a) vs $\alpha_s$ for 500-eV Ar-ion bombardment of vacuum-fractured $SrTiO_3$(100) surface. See text for explanation of dashed lines in (b).

shown in Figs. 3(b)–3(d) for bombardment times of 10, 30, 90, and 600 sec. The solid curves correspond to the photoemission spectra in Fig. 4; the dashed curve for 30-sec bombardment time has been added to show the changes that occur between 10 and 30 sec. With ion bombardment the features at 7.0 and 10.5 eV disappear, and the feature initially at 5.5 eV broadens and shifts slightly toward higher energy. In the region just below the elastic peak (1 eV $< E_L <$ 3 eV), $dn(E)/dE$ first increases (10 sec); then a distinct peak at $E_L = 2.2$ eV appears (30 sec), grows slightly (90 sec), and then remains nearly constant under further bombardment. The 2.2-eV peak appears just at $\alpha_s = 1$, as does the similar energy-loss peak in $TiO_2$.[6] In $TiO_2$, however, the low-energy loss peak grows continuously with ion bombardment until it is the dominant feature in the loss spectrum. We have attributed this peak in $TiO_2$ to the formation of pairs in $Ti^{3+}$ ions that share a common face of the O octahedra. The $TiO_2$ lattice contains planes of empty sites into which Ti ions can move to produce such a pairing. Although the $SrTiO_3$ lattice does not have the proper type of empty sites, we believe that the 2.2-eV energy-loss peak in $SrTiO_3$ also arises from that type

of pairing (see Sec. V below).

The electronic structure of the surface of $SrTiO_3$ is quite sensitive to the conditions of surface treatment. For example, when a $SrTiO_3(100)$ surface was bombarded with Ar ions of 260, 500, or 1000 eV until no further changes were seen in any of the electron spectra, the same relative Auger peak heights for the three elements were observed in each case, and yet the photoemission and energy-loss spectra were noticeably different. Figure 8 shows the photoemission spectra obtained from an annealed (100) surface after bombardment at each of the three ion energies. After 260-eV bombardment, a few faint, broad LEED spots were still visible, and the two peaks in the valence-band emission are still resolved. The spectra after bombardment with 500- and 1000-eV ions are similar to each other, but the valence band is narrower at the higher bombardment energy. The widths of the valence band for the annealed surface and for the surface after bombarding with 260-, 500-, and 1000-eV ions are 6.2, 6.1, 5.8, and 5.6 eV, respectively. (While a determination of the width of the valence-band emission is somewhat subjective, the differences between the various widths are accurate to 0.1 eV.) The corresponding energy-loss spectra are shown in Fig. 9. The 7.0- and 10.5-eV loss peaks are still present after 260-eV bombardment, consistent with the presence of some LEED structure. The 2.2-eV loss peak is just beginning to appear after 500-eV bombardment; its amplitude is much smaller than on the vacuum-fractured surfaces that were bombarded at the same energy (Fig. 3). After bombardment at 1000 eV, the 2.2-eV peak is larger than in Fig. 3. Because of this sensitivity to surface treatment we have restricted most of our experiments to a single bombardment energy (500 eV) in order to minimize the number of variables. The 2.2-eV energy-loss peak is particularly sensitive to surface treatment, and we have not made the quantitative use of it here that we did in our studies of $TiO_2$.[6]

### B. Annealing of bombarded surfaces

When $TiO_2(110)$ surfaces are annealed after ion bombardment, O diffuses from the bulk to restore the

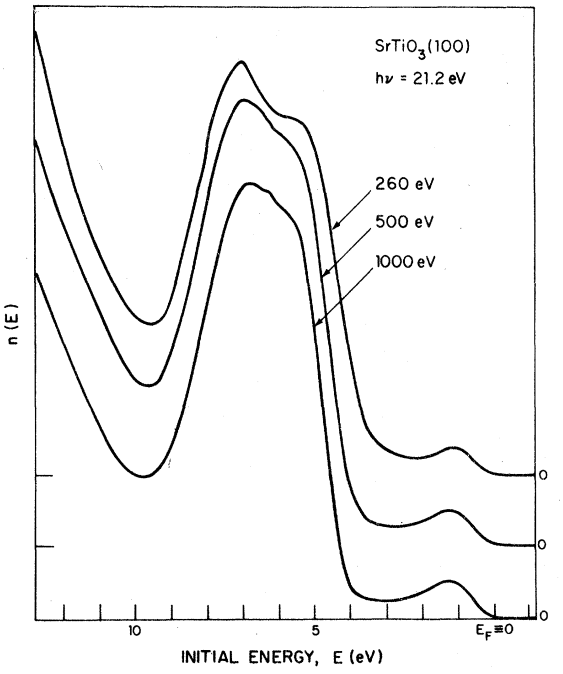


FIG. 8. UPS spectra for $SrTiO_3(100)$ after Ar-ion bombardment to equilibrium at ion energies shown.

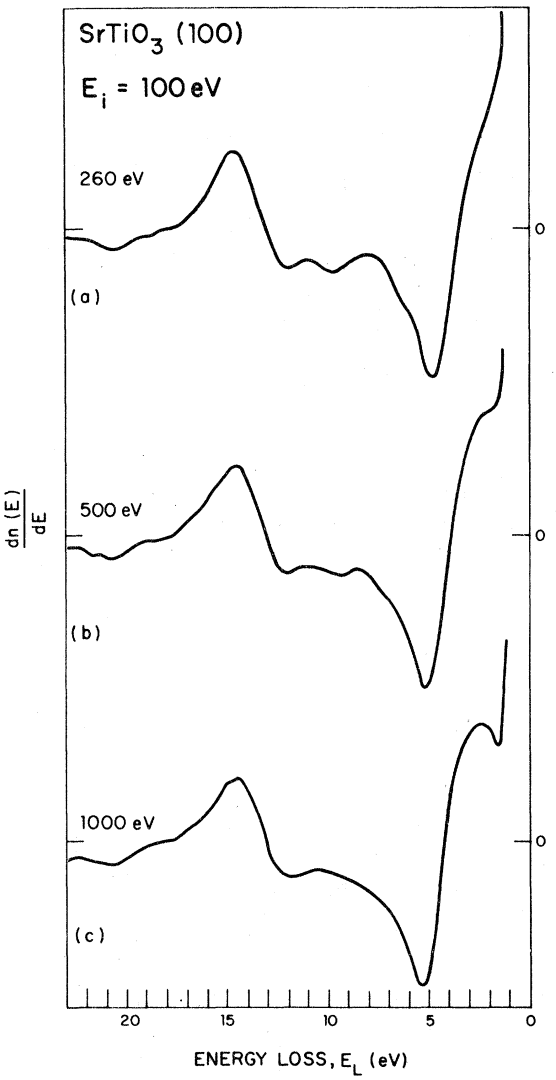


FIG. 9. Energy-loss spectra for $SrTiO_3(100)$ after Ar-ion bombardment to equilibrium at ion energies shown.

O that was removed by bombardment.[6] Excellent LEED patterns result, the band-gap surface state disappears, and the surface appears to be a nearly perfect $TiO_2(110)$ surface. When ion-bombarded $SrTiO_3(100)$ surfaces are heated to about 1200 K for a few minutes, fairly good $(1\times1)$ LEED patterns result, but there is very little change in the Auger spectra. In fact, the Sr-to-Ti and O-to-Ti Auger peak ratios decrease by an additional 10%–15% after annealing compared to the values for the ion-bombarded surface. Although O is known to diffuse from the bulk of $SrTiO_3$ at that temperature,[7] diffusion does not appear to restore the O ions missing from the surface layer. This suggests that the surface structure produced by ion bombardment may be a stable phase up to 1200 K, and that it may just order to give good LEED patterns. Figure 10(a) shows the photoemission spectrum from an Ar-ion-bombarded $SrTiO_3(100)$ surface, with the amplitude in the band-gap region expanded by a factor of 16. Figure 10(b) shows the spectrum obtained after the surface had been heated to about 1200 K for a few minutes. The valence-band emission shows two peaks similar to those from a vacuum-fractured surface (Fig. 2), and the width of the valence band has increased, as discussed in Sec. IV A above. The band-gap emission peak has narrowed from 1.5-eV full width at half-maximum (FWHM) after bombardment to 1.0 eV after subsequent annealing, but the total area under the peak is essentially the same. This suggests that the total number of $Ti^{3+}$ ions has not changed, but that annealing has placed most of them in the same ligand environment. A sharp feature also appears near $E=17$ eV after annealing [Fig. 10(b)], while the ion-bombarded surface only exhibits a shoulder there. Since that feature is very close to the cutoff of the spectrum imposed by the vacuum level, it may be the beginning of a peak that lies more than 17 eV below $E_F$. Such a peak could be due to the Sr(4$p$) band (see Fig. 1), but since the feature is not present on fractured surfaces it may instead be a characteristic of the ordered, nonstoichiometric surface layer.

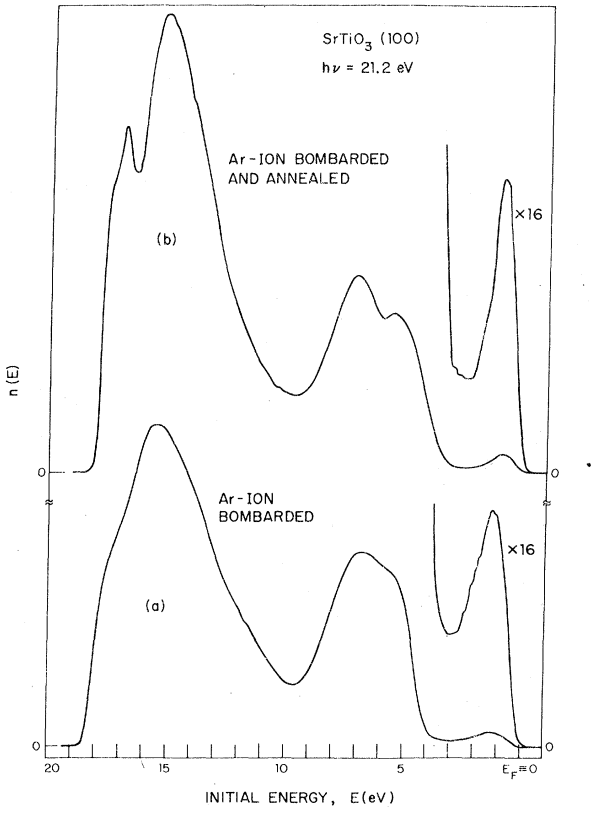


FIG. 10. UPS spectra for (a) Ar-ion bombarded $SrTiO_3(100)$ and (b) surface in (a) after annealing.

### C. Interaction of $O_2$ with defect surface states

We have also studied the effects of $O_2$ adsorption on the electronic structure of $SrTiO_3$ surfaces.[16] Figure 11(a) shows the photoemission spectra for a (100) surface heavily bombarded with 500-eV Ar ions ($\alpha_s>3$) before (solid curve) and after (dashed curve) exposure to $10^8$ L $O_2$ at room temperature. For ease of comparison, the two curves have been aligned at the top edge of the valence band $E_v$ and initial-state energy is referenced from that point. The band-gap surface-state peak completely disappears after exposure to $O_2$ and the valence-band emission increases. A shoulder also appears at $E\approx8$ eV; it is believed to arise from the presence of chemisorbed $O_2$ at large $O_2$ exposures.[16] Figure 11(b) shows, on an expanded vertical scale, the emission from the band-gap region of the surface that was exposed to $10^8$ L $O_2$, corrected by subtraction of the "ghost" valence-band emission generated by the 23.1 eV He line. The subtraction procedure is the same one used to obtain Fig. 2(b) for the vacuum-fractured surface. There is no trace of either the band-gap surface-state emission that results from ion bombardment or the peak that occurs near midgap on the fractured surface [Fig. 2(b)]; there is only a smooth tailing off of emission into the gap.

Figure 12 shows the change in the work function and the positions of the Fermi level and the band-gap surface-state peak that occured when two of the surfaces used in Figs. 5–7 were exposed to $O_2$ [after having been bombarded to equilibrium ($\alpha_s>3$)]. The exposures ranged from 0.5 to $10^8$ L, and $\alpha_s$ was found to vary with exposure roughly as

$$\ln\alpha_s=0.10-0.58\ln L\ , \tag{5}$$

where $L$ is the exposure in langmuirs. The solid lines in Fig. 12 are least-squares linear fits to the data for $\alpha_s>0.5$. The data do not exhibit the sharp slope changes that were seen on initial bombardment of fractured surfaces; this is consistent with the results

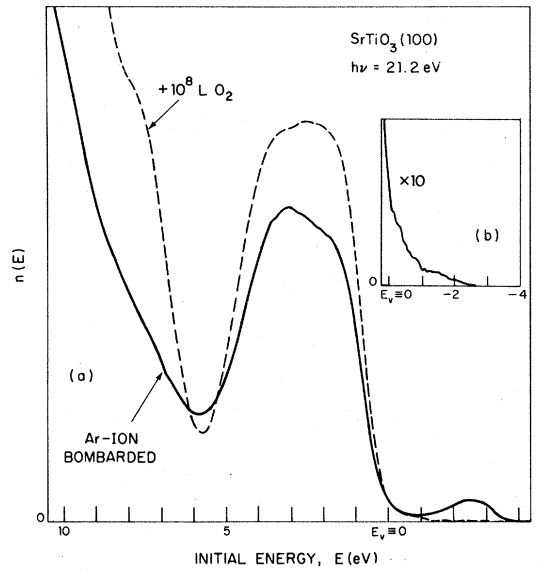


FIG. 11. (a) UPS spectra for Ar-ion bombarded $SrTiO_3(100)$ before (solid curve) and after (dashed curve) exposure to $10^8$ L $O_2$. (b) Band-gap region after $O_2$ exposure, with 23.1-eV "ghost" spectrum subtracted.

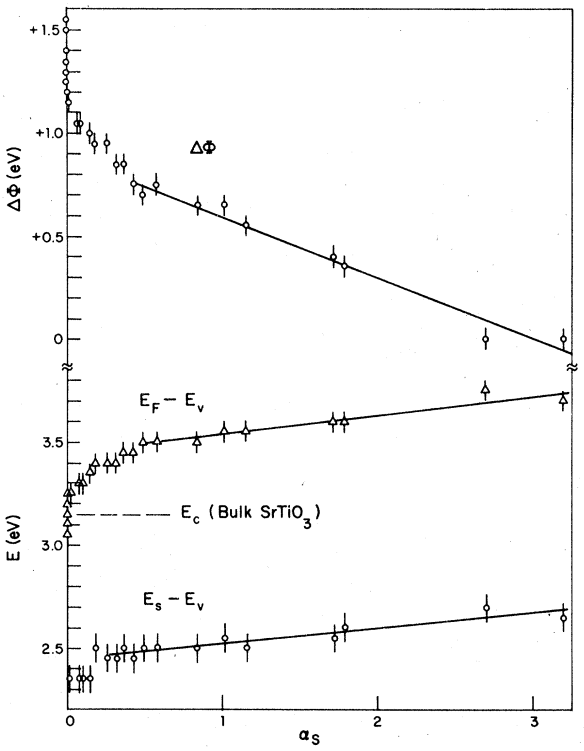


FIG. 12. Work-function change ($\Delta\Phi$), Fermi level ($E_F - E_v$), and position of UPS surface-state peak ($E_s - E_v$) vs $\alpha_s$ for $O_2$ adsorption on Ar-ion bombarded $SrTiO_3(100)$.

on $TiO_2$.[6] The photoemission intensity from the band-gap surface state goes to zero (i.e., $\alpha_s = 0$) by an exposure of $10^4$ L, but further exposure causes additional changes in $\Delta\Phi$ and $E_F$, as indicated by the data points lying along the $\alpha_s = 0$ axis. The peak in the band-gap emission moves toward the valence band with $O_2$ exposure at about the same rate as does the Fermi level, remaining 1.0 eV below $E_F$. The work function rises by 1.15 eV before the band-gap emission has disappeared, and it rises another 0.4 eV for exposures of $10^4$ to $10^8$ L.

The energy-loss spectra for 500-eV Ar-ion-bombarded $SrTiO_3(100)$ before (solid curve) and after (dashed curve) exposure to $10^8$ L $O_2$ are shown in Fig. 13. For this particular surface there is no 2.2-eV loss peak, even though the surface was bombarded to equilibrium and the photoemission spectrum looked the same as for surfaces that did exhibit the energy-loss peak. Exposure to $O_2$ reduces the intensity in $dn(E)/dE$ just below the elastic peak (1 eV $< E_L <$ 3 eV), shifts the first major loss feature back to its position on a fractured surface, and gives two additional peaks at $E_L = 8.1$ and 10.8 eV; the fourth peak occurs at 13.6 eV after $O_2$ exposure. Qualitatively, this spectrum looks very much like that from a fractured surface [Fig. 3(a)], but the peak locations are slightly different. (We were unable to obtain meaningful Auger spectra from surfaces exposed to $O_2$ because of electron-stimulated desorption of adsorbed O by the 2000-eV electron beam.)

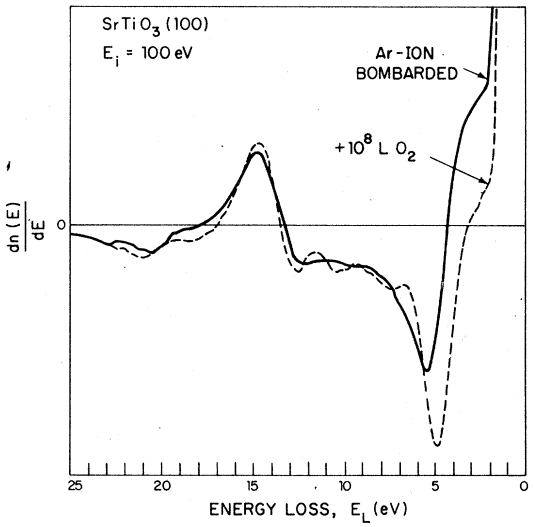


FIG. 13. Energy-loss spectra for Ar-ion bombarded $SrTiO_3(100)$ before (solid curve) and after (dashed curve) exposure to $10^8$ L $O_2$.

The response of differently prepared $SrTiO_3(100)$ surfaces to $O_2$ exposure is shown in Fig. 14, where the work function $\Phi$ (not $\Delta\Phi$) and the locations of the Fermi level and the band-gap surface-state peak are plotted vs exposure in Langmuir. This abscissa was used instead of $\alpha_s$ since $\alpha_s$ goes to zero at exposures of about $10^4$ L. The open circles are for a surface bombarded with 1000-eV Ar ions, the solid circles and triangles for two surfaces bombarded with 500-eV Ar ions, and the open triangles for a surface that was annealed after bombardment with 500-eV Ar ions. All quantities are seen to depend strongly on initial surface treatment. It is interesting to note that the differences in $(E_F - E_v)$ for the various surfaces in Fig. 14 are the same as the differences in width of the valence band seen in Figs. 8 and 10 for those surfaces. It thus appears that, for the same $O_2$ exposure, the location of $E_F$ for all of the surfaces is the same with respect to the *bottom edge* of the valence band.

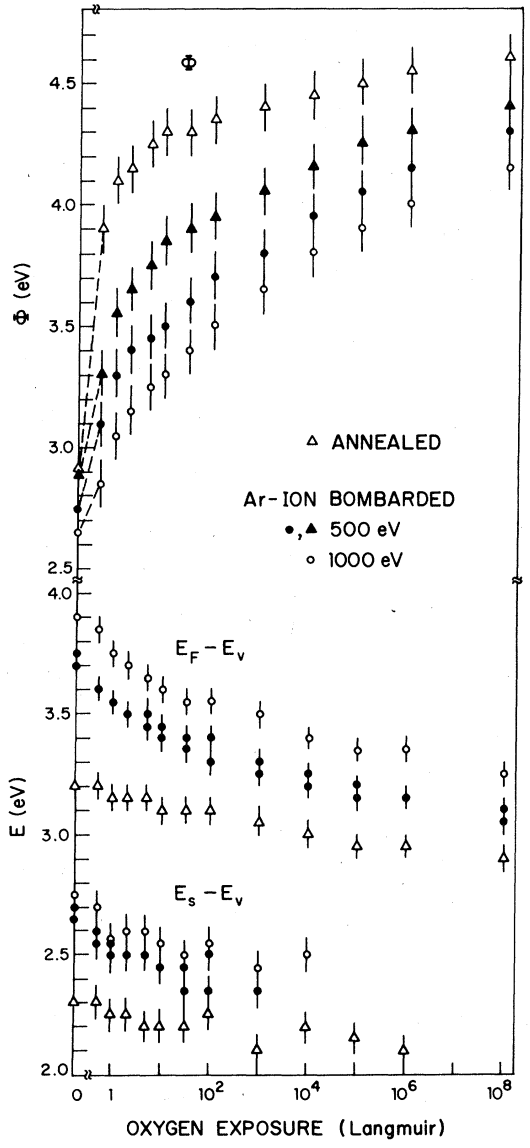


FIG. 14. Work function ($\Phi$), Fermi level ($E_F - E_v$), and position of UPS surface-state peak ($E_s - E_v$) vs $O_2$ exposure for various $SrTiO_3(100)$ surfaces.

## V. DISCUSSION

### A. Surface states on vacuum-fractured $SrTiO_3$

Due to the modified potential at the surface of a crystal, the electronic states associated with the surface are shifted relative to the bulk states. These intrinsic surface states form two-dimensional electronic bands whose widths in energy should be similar to those of the bulk electronic bands. Wolfram and co-workers have considered these two-dimensional bands in detail for $SrTiO_3$. Their initial calculations[1,2] show the *d*-electron surface states on an ideal (100) surface to be shifted down into the bulk band gap by about 1.5 eV. In reduced $SrTiO_3$, where the Fermi level lies near the bottom of the bulk conduction band, such surface states would be largely occupied (with a density of about $10^{15}$ electrons/cm$^2$) and should be easily detected in a photoemission experiment. However, when Powell and Spicer[3] examined reduced, vacuum-fractured $SrTiO_3$, they found a maximum surface-state density in the bulk band-gap region of only $10^{13}$ electrons/cm$^2$. Henrich *et al.*[6] found similar results for reduced $TiO_2(110)$, as did Chung *et al.*[17] for $TiO_2(110)$, (100) $[1\times3]$, and (100) $[1\times5]$. Wolfram and Ellialtioğlu[4] then extended the calculations to include the effect of Coulomb repulsion among the *d* electrons and found that a "surface-enhanced covalency" pushes the surface states up toward, and even into, the region of the bulk conduction band as the Fermi level is moved up toward the conduction-band edge. The intrinsic surface states would thus be largely empty regardless of the position of the Fermi level, in agreement with the photoemission experiments.

The photoemission spectra for vacuum-fractured-reduced $SrTiO_3$ reported here are in general agreement with previous measurements on $SrTiO_3$ in that a relatively small density of occupied states is seen in the region of the bulk band gap. There are detailed differences between the various measurements, however. In photoemission spectra that we have taken on about 20 different fractured surfaces, the amplitude of the peak in the band-gap emission varies by a factor of 3 to 4. The smallest amplitude corresponds to a surface-state density of about $5\times10^{13}$ electrons/cm$^2$. Powell and Spicer[3] studied two fractured surfaces, one on each of two different samples. They found a large difference in the intensity of the band-gap emission between the two samples, with the stronger emission

corresponding to a surface-state density of about $1 \times 10^{13}$ electrons/cm$^2$. The band-gap emission tailed off smoothly from the valence band, rather than exhibiting a peak. (Since an ultraviolet monochromator was used in those measurements, no corrections were necessary for "ghost" lines.) Derbenwick[11] has also studied the ultraviolet photoemission spectra from vacuum-fractured $SrTiO_3(100)$. Although he was not expressly looking for surface states, his quantum yield curves show band-gap emission with an amplitude 5–10 times larger than that seen by Powell and Spicer, putting it in the range seen in the present experiments. Derbenwick's quantum yield curves also exhibit more structure in the band-gap region than do those of Powell and Spicer, although this region was not studied in detail at large photon energies.

The wide variation in the band-gap emission from different fractured $SrTiO_3(100)$ surfaces suggests that the emission arises primarily from extrinsic surface states (i.e., surface defects) rather than intrinsic states. Such an interpretation is consistent with the LEED patterns observed in the present experiment as well as with the behavior of the band-gap emission upon exposure to $O_2$.

### B. Changes in surface structure due to ion bombardment

For ion-bombarded $SrTiO_3$ in the region $\alpha_s < 1$, the surface becomes disordered, as evidenced by the degradation of LEED patterns, without a change in surface composition. The surface states that appear in the bulk band-gap region are necessarily associated with the disorder. We believe that they arise from $Ti^{3+}$–O-vacancy complexes similar to those postulated for $TiO_2$.[6] All Sr levels, either filled or empty, are sufficiently far in energy from the band gap (see Fig. 1) that they should not contribute to occupied surface states in the band-gap region; this assumption is made in the calculation of the electronic structure of $SrTiO_3$ surfaces.[1] An electron trapped at a $Ti^{3+}$–O-vacancy complex may be associated primarily with one Ti ion, or it may be shared by two adjacent Ti ions, depending on the details of the complex.

During the initial stages on ion bombardment of $TiO_2$, the photoemission intensity from the band-gap surface states increases without any change in the position of these states relative to the upper edge of the valence band $E_v$.[6] In $SrTiO_3$, on the other hand, the defect surface-state band created at low ion doses moves away from $E_v$ by 0.3–0.4 eV as $\alpha_s$ increases from 0 to 1. If the position of the band-gap surface state is referred to either the bottom of the valence band or to $E_F$, however, both $TiO_2$ and $SrTiO_3$ behave in a similar manner. There is a theoretical basis for referring the position of the band-gap surface state to the Fermi level. The defect surface states produced by ion bombardment are largely derived from the Ti($3d$) conduction band of $SrTiO_3$ or $TiO_2$, and for small $\alpha_s$ in $n$-type samples $E_F$ is located near the bottom edge of that band. To the extent that the properties of the surface bands do not change and that the defects do not interact (i.e., $\alpha_s \ll 1$), $E_F - E_s$ should remain constant. In fact, as $\alpha_s$ increases from 0 to 1, $E_F - E_s$ increases by about 0.15 eV for $SrTiO_3$ and by about 0.20 eV for $TiO_2$, both small fractions of $E_F - E_v$.

At $\alpha_s = 1$ a phase transition occurs, accompanied by a number of changes in the physical and electronic properties of the surface. At that point the sample has been hit by an average of about one Ar ion per surface unit cell (as determined from measured ion-beam parameters), so the defect density is probably large enough that the defects begin to interact with each other. The surface structure destabilizes, and ion bombardment now removes both Sr and O from the surface more rapidly than Ti. The 2.2-eV energy-loss peak is only observed for $\alpha_s > 1$, but because it is weak and nonreproducible we do not believe that it is intrinsic to the new surface phase; we will discuss its origin below. For $\alpha_s > 1$ the width of the valence band remains constant, as does $E_F - E_v$. The rate of increase of $E_s - E_v$ with increasing $\alpha_s$ is 3.5 times slower for $\alpha_s > 1$ than for $\alpha_s < 1$.

When $TiO_2$ is bombarded with Ar ions, the equilibrium surface structure that results for long bombardment times is essentially $Ti_2O_3$.[6] Since the structural and electronic properties of $Ti_2O_3$ are well known, it is possible to infer the detailed nature of the changes that take place on the surface of $TiO_2$ as a result of bombardment.[6] For $SrTiO_3$, however, ion bombardment does not result in such a well defined final state. Using a continuum model, the equilibrium surface composition that is reached after long ion-bombardment times ($\alpha_s \sim 3$) was determined in Sec. IV A to be roughly $SrTi_2O_4$, independent of ion energy over the available range of 260 to 1000 eV. Although bulk $SrTi_2O_4$ has been prepared,[18] little is known about its electronic properties, and its crystal structure is sufficiently different from that of $SrTiO_3$ that we do not believe it to be the surface phase that results from ion bombardment of $SrTiO_3$.

We can get some insight into the detailed structure of bombarded and annealed $SrTiO_3(100)$ surfaces, however. The fact that they exhibit good LEED patterns, while remaining Sr and O deficient, suggests considering model surface structures with given atomic arrangements and calculating the Auger peak amplitudes that would be expected from such structures. This is done by simply adding up the contributions to the Auger spectra from each plane of atoms, including the attenuation of the primary electron beam, the electron mean-free path, and the spectrometer collection geometry. The short electron mean-free paths mean that small changes in the uppermost layer of atoms make significant changes in the Auger spectra.

For example, in the [100] direction, $SrTiO_3$ is built up of two different planes of atoms, a densely packed layer containing one Ti and two O atoms per surface unit cell (a Ti-$O_2$ plane) and a more open plane containing one Sr and one O atom per unit cell (a Sr-O plane). A fractured surface will contain equal areas of Ti-$O_2$ and Sr-O planes as the uppermost layer, and so the Sr-to-Ti and O-to-Ti Auger ratios in Fig. 6 are normalized to unity for such a combination of planes. If only Ti-$O_2$ planes were present as the top layer, the Auger spectra would exhibit a relatively stronger Ti peak; the computed ratios, normalized to the fractured surface, are 0.54 for Sr-to-Ti and 0.90 for O-to-Ti. A surface that terminated solely in Sr-O planes, on the other hand, would give a relatively stronger Sr Auger peak; the computed ratios there are 1.68 for Sr-to-Ti and 1.15 for O-to-Ti.

The Auger ratios seen for an ion-bombarded and annealed $SrTiO_3(100)$ surface are thus close to those for a pure Ti-$O_2$ surface, the Sr-to-Ti ratio being exactly the same. The relatively open Sr-O planes are probably removed much more readily by ion bombardment than the Ti-$O_2$ planes, resulting in a surface that is predominantly Ti-$O_2$. The O-to-Ti ratio could be further lowered by removing some O atoms from the top plane. The UPS spectra for vacuum-fractured $SrTiO_3(100)$ (Sec. III) indicate that a perfect Ti-$O_2$ surface plane will not exhibit appreciable band-gap emission even though the Ti ions are missing one O ligand. Some type of defect in a Ti-$O_2$ surface is therefore necessary to populate the Ti($3d$) levels and create the observed surface states. Removing an $O^{2-}$ ion in the form of a neutral O atom would leave two electrons behind that could populate the Ti($3d$) states. If we assume a localized ionic model in which charge transfer is restricted to the top atomic plane, then all of the Ti ions could be converted to a $Ti^{3+}(3d^1)$ configuration by removing 25% of the $O^{2-}$ ions. Such a surface would give Auger ratios of 0.54 for Sr-to-Ti and 0.81 for O-to-Ti, consistent with Fig. 6. In order to obtain (100) [1 × 1] LEED patterns, the O vacancies would have to be randomly distributed; a regular ordering of defects would give rise to additional LEED spots.

The UPS data for ion-bombarded and annealed $SrTiO_3$ provide additional support for the localized model of the bombarded and annealed surface presented above. Because of the small escape depth of photoelectrons, UPS spectra give only the position of the valence-band edge $E_v$ in the first 10–20 Å of the sample. Since $E_F$ lies very close to the bottom edge of the conduction band in the bulk, $(E_F - E_v) - E_{gap}$ is a measure of the (downward) band bending which occurs in the sample due to the presence of surface states. The UPS spectra for ion-bombarded and annealed $SrTiO_3$ (Fig. 10) show essentially zero band bending (within the experimental error of ±0.05 eV). This is consistent with the conclusion that the band-gap surface states arise from localized $Ti^{3+}$–O-vacancy defects in the surface layers, with the $Ti^{3+}$ $d$ electrons provided by the O that is removed from the surface by ion bombardment. On the other hand, if an appreciable fraction of the $d$ electrons were supplied from the $SrTiO_3$ bulk, the resulting depletion layer would have produced significant band bending. It should be noted that an itinerant-electron model has recently been considered by Ellialtioğlu *et al.*[19] to explain the photoemission spectra from bombarded and annealed $SrTiO_3$ surfaces.

We have considered other atomic arrangements for the surface structure of ion-bombarded and annealed $SrTiO_3(100)$, but the one described above fits more of the experimental data. One difficulty with this model, however, is the observation that the UPS spectra exhibit a negligible density of states at the Fermi level. In a band interpretation, this would imply that the surface states consist of a filled band derived from Ti($3d$) states and separated by a gap from higher-lying Ti($3d$)-derived bands. But it is difficult to see how such a filled band could arise without an interaction like the Ti-Ti pairing that occurs in $Ti_2O_3$.[20] Such a pairing would give rise to superstructure in the LEED patterns for this surface, which is not observed. A possible solution to this dilemma is to assume that the $Ti^{3+}$–O-vacancy surface states remain localized in spite of their high density.

The structure of ion-bombarded $SrTiO_3(100)$ surfaces that have *not* been annealed is not amenable to the application of atomic models such as those discussed above for annealed surfaces. The absence of LEED patterns indicates that at least the first 3 or 4 atomic planes of the sample must be disordered. It is then possible either that the stoichiometry of that whole region could have changed (hence the application of a continuum model of the surface structure in Sec. IV A above) or that atomic vacancies are confined to the top plane and that several planes below are disordered without a change in atomic composition. The rapid depopulation of the surface states on bombarded surfaces with $O_2$ exposure (Fig. 12) suggests that the $d$-electrons are confined to the uppermost atomic layer, but a migration of O ions into the sample, in a manner similar to the oxidation of Sr,[21] and of Cs,[22] cannot be ruled out. None of these models provide a satisfactory explantion of the surface-phase transition that occurs at $\alpha_s = 1$.

The small amplitude and nonreproducibility of the 2.2-eV energy-loss peak suggest that it is not intrinsic to the surface phases that are produced by ion bombardment. A similar but large and reproducible peak in $Ti_2O_3$ and Ar-ion-bombarded $TiO_2$ is believed to arise from transitions between bonding and antibonding levels of pairs of $Ti^{3+}$ ions that interact across the common faces of neighboring oxygen octahedra.[6] The perovskite structure does not contain sites that could accomodate such pairs, however.[23] We have found

that in a few instances where Ar-ion bombarded and annealed $SrTiO_3(100)$ surfaces exhibit streaking between diffraction spots, indicating a tendency toward faceting or step formation on the surface, they also exhibit particularly strong 2.2-eV energy-loss peaks. This suggests that the energy-loss peak may be due to a particular property of step sites. If $Ti^{3+}$ ions were to be trapped at step site on a (100) surface consisting predominantly of $Ti\text{-}O_2$ planes, the interaction of those trapped ions with the $Ti^{3+}$ ions in normal octahedral lattice sites would be similar to the $Ti^{3+}$ pairing that occurs in $Ti_2O_3$. The local environment would consist of three O ions in a plane between two $Ti^{3+}$ ions and normal to the pair axis; this environment could probably provide sufficient screening of the $Ti^{3+}$-$Ti^{3+}$ Coulomb repulsion to produce pairing and to stabilize the bonding and antibonding orbitals of the $Ti^{3+}$ ions.

It is also possible that the presence of $Ti^{3+}$ ions trapped at a small number of step sites on fractured surfaces could be responsible for the weak band-gap photoemission peak observed for those surfaces. That peak is about 0.5 eV closer to the valence band than is the defect surface state produced by ion bombardment near $\alpha_s = 0$, consistent with a different structural nature of the defects in the two cases.

## VI. SUMMARY

The surface electronic properties of vacuum-fractured, Ar-ion-bombarded, and annealed $SrTiO_3$ have been studied; they are found to be similar in many respects to those of $TiO_2$, which we have previously reported. Vacuum-fractured surfaces with orientations close to (100) exhibit a weak photoemission peak in the region of the bulk band gap, which is probably due to an extrinsic surface state resulting from residual surface defects. When surface defects are produced by Ar-ion bombardment, changes occur in the electronic structure of the valence band, and a band of defect surface states appears in the region of the bulk band gap. Two distinct surface-defect phases are seen as the density of defects is varied. These surface states arise from the creation of $Ti^{3+}$ ions on the surface and are predominantly of *d*-electron character. The surface first disorders under ion bombardment and then loses O and Sr, finally reaching a stable surface composition at long bombardment times. That composition is stable even when the surface is reordered by annealing. An ionic model involving O vacancies in $Ti\text{-}O_2$ surface planes is able to account for much of the experimental data.

When $SrTiO_3$ surfaces are exposed to $O_2$, the defect surface states disappear from the photoemission spectra, presumably because of the formation of a more complete O-coordination of the surface Ti ions. This is true for the small density of defects that are present on vacuum-fractured surfaces as well as for those defects produced by ion bombardment.

## ACKNOWLEDGMENTS

The authors thank T. Wolfram, J. B. Goodenough, and E. I. Solomon for many enlightening discussions, E. B. Owens for performing the mass spectrographic analysis, and B. Feldman for technical assistance. This work was sponsored by the Department of the Air Force.

*Present address: Francis Bitter National Magnet Laboratory, MIT, Cambridge, Mass. 02139.

[1]T. Wolfram, E. A. Kraut, and F. J. Morin, Phys. Rev. B 7, 1677 (1973).

[2]F. J. Morin and T. Wolfram, Phys. Rev. Lett. 30, 1214 (1973).

[3]R. A. Powell and W. E. Spicer, Phys. Rev. B 13, 2601 (1976).

[4]T. Wolfram and Ş. Ellialtioğlu, Appl. Phys. 13, 21 (1977).

[5]V. E. Henrich, G. Dresselhaus, and H. J. Zeiger, Bull. Am. Phys. Soc. 22, 364 (1977).

[6]V. E. Henrich, G. Dresselhaus, and H. J. Zeiger, Phys. Rev. Lett. 36, 1335 (1976).

[7]H. Yamada and G. R. Miller, J. Solid State Chem. 6, 169 (1973).

[8]S. M. Sze, *Physics of Semiconductor Devices* (Wiley-Interscience, New York, 1969), p. 370.

[9]K. W. Blazey, Phys. Rev. Lett. 27, 146 (1971).

[10]D. M. Tench and D. O. Raleigh, *Electrocatalysis on Non-Metallic Surfaces,* Natl. Bur. Stand. Spec. Publ. No. 455 (U.S. GPO, Washington, D. C., 1976), p. 229.

[11]G. F. Derbenwick, Ph.D. thesis (Stanford University, 1970) (unpublished).

[12]J. C. Tracy, NATO Summer School Lectures, Ghent, Belgium, 1972, (unpublished); C. R. Brundle, J. Vac. Sci. Technol. 11, 212 (1974).

[13]Similar effects have been reported in $TiO_2$; see, S. Thomas, Surf. Sci. 55, 754 (1976).

[14]P. W. Palmberg, Anal. Chem. 45, 549A (1973).

[15]Similar changes have been reported in $TiO_2$ [M. L. Knotek (unpublished)].

[16]H. J. Zeiger, V. E. Henrich, and G. Dresselhaus, Bull. Am. Phys. Soc., Ser. II 22, 419 (1977); V. E. Henrich, G. Dresselhaus, and J. J. Zeiger, J. Vac. Sci. Technol. (to be published).

[17]Y. W. Chung, W. J. Lo, and G. A. Somorjai, Surf. Sci. 64, 588 (1977).

[18]O. Muller and R. Roy, *The Major Ternary Structural Families* (Springer-Verlag, Berlin, 1974), p. 274.

[19]Ş. Ellialtioğlu, T. Wolfram, and V. E. Henrich (unpublished).

[20]J. B. Goodenough, in *Progress in Solid State Chemistry,* edited by H. Reiss (Pergamon, New York, 1972), p. 233.

[21]C. R. Helms and W. E. Spicer, Phys. Rev. Lett. 32, 228 (1974).

[22]P. E. Gregory, P. Chye, H. Sunami, and W. E. Spicer, J. Appl. Phys. 46, 3525 (1975).

[23]J. B. Goodenough, in Ref. 20, p. 216.